

Interannual observations and quantification of summertime H₂O ice deposition on the Martian CO₂ ice south polar cap

Adrian J. Brown^{*1}, Sylvain Piqueux², Timothy N. Titus³

¹ SETI Institute, 189 Bernardo Ave, Mountain View, CA 94043, USA

² Jet Propulsion Laboratory, California Institute of Technology, 4800 Oak Grove Drive, Pasadena, CA 91109 USA

³ U.S. Geological Survey, Astrogeology Science Center, Flagstaff, AZ 86001 USA

Abstract

The spectral signature of water ice was observed on Martian south polar cap in 2004 by the *Observatoire pour l'Mineralogie, l'Eau les Glaces et l'Activite* (OMEGA) (Bibring et al., 2004). Three years later, the OMEGA instrument was used to discover water ice deposited during southern summer on the polar cap (Langevin et al., 2007). However, temporal and spatial variations of these water ice signatures have remained unexplored, and the origins of these water deposits remains an important scientific question. To investigate this question, we have used observations from the Compact Reconnaissance Imaging Spectrometer for Mars (CRISM) instrument on the Mars Reconnaissance Orbiter (MRO) spacecraft of the southern cap during austral summer over four Martian years to search for variations in the amount of water ice.

We report below that for each year we have observed the cap, the magnitude of the H₂O ice signature on the southern cap has risen steadily throughout summer, particularly on the west end of the cap. The spatial extent of deposition is in

* corresponding author, email: abrown@seti.org

disagreement with the current best simulations of deposition of water ice on the south polar cap (Montmessin et al., 2007).

This increase in water ice signatures is most likely caused by deposition of atmospheric H₂O ice and a set of unusual conditions makes the quantification of this transport flux using CRISM close to ideal. We calculate a 'minimum apparent' amount of deposition corresponding to a thin H₂O ice layer of 0.2mm (with 70% porosity). This amount of H₂O ice deposition is 0.6-6% of the total Martian atmospheric water budget. We compare our 'minimal apparent' quantification with previous estimates.

This deposition process may also have implications for the formation and stability of the southern CO₂ ice cap, and therefore play a significant role in the climate budget of modern day Mars.

Highlights

- We report on the H₂O ice depositional cycle on the Martian CO₂ ice residual south polar cap
- We use data from the CRISM instrument obtained over the past four Martian summer periods
- Potential models: 1) cold trapping 2) sublimation 3) entrained H₂O ice in sublimation flow
- The 'minimal apparent' amount of water ice deposited corresponds to a layer 0.2mm thick.

Brown et al.

- This amounts to over 0.6-6% of the total Martian atmospheric water budget.

Corresponding author:

Adrian Brown

SETI Institute

189 Bernardo Ave, Mountain View, CA 94043

ph. 650 810 0223

fax. 650 968 5830

email. abrown@seti.org

Short running title: “Observations of the H₂O ice cycle on summertime Martian south pole”

KEYWORDS

Mars, south pole, H₂O ice, CO₂ ice, ices, snow, snowpack, grain size, radiative transfer

1. Introduction

The Martian north polar ice cap has long been understood as the most important exposed source and sink of water on modern day Mars (Farmer et al., 1976). In contrast, the south seasonal cap was thought to be essentially composed of CO₂ ice following surface temperature measurements using the Viking Infrared Thermal Mapper (IRTM) (Kieffer, 1979). In the late 1990s, the Mars Global Surveyor Thermal Emission Spectrometer (TES) also confirmed CO₂ ice temperatures in the south pole residual cap (SPRC) during the austral summer (Kieffer et al., 2000) and found “no significant presence” of H₂O ice. Soon after this observation, Nye et al. (2000) published an influential theoretical paper showing that a pure CO₂ ice south polar cap would collapse under its own weight, and suggested dirty H₂O ice as the principle ice cap constituent. In 2004, the OMEGA instrument on Mars Express was used for one Earth month to observe the Martian south polar region from L_s=335-348 and reported observations of H₂O ice mixed with CO₂ ice in the residual south polar cap and polar layered deposits (Bibring et al., 2004). Doute et al. (2006) used OMEGA to examine the water and dust content of the south polar cap during late summer. Langevin et al. (2007) mapped the springtime retreat and summer evolution of the south polar cap and were the first to note the deposition of water ice on the south polar cap.

Further complicating this cap compositional picture, large deposits of CO₂ ice have recently been discovered in the subsurface of the south polar layered deposits (Phillips et al., 2011).

Viking IRTM and TES temperature observations show that CO₂ ice is the predominating ice in the surface/near surface in the residual cap during summer (Kieffer, 1979; Titus et al., 2008). Mars Global Surveyor Mars Orbiter Camera (MOC) images of the south polar cap were used to discover 'Swiss cheese features' (Malin et al., 2001) which were successfully modeled as a meters-thick layer of CO₂ ice underlain by H₂O ice (Byrne and Ingersoll, 2003). Mars Odyssey Thermal Imaging Spectrometer (THEMIS) temperature observations of the south polar cap have been used to infer that H₂O ice becomes exposed at the periphery of the residual cap during late summer (Piqueux et al., 2008), and Titus et al. (2003) used thermal and visual observations, combined with subpixel mixing models, to identify a possible H₂O ice lag at the edge of the gullies and trenches in the SPRC that were exposed as the edge of the retreating seasonal CO₂ ice cap moved poleward during summer. However, THEMIS and TES do not have spectral coverage of near-infrared (NIR 1.0-2.5 μm) region of the electromagnetic (EM) spectrum where several CO₂ and H₂O ice absorption bands are available to CRISM.

CRISM is very sensitive to water ice deposited on the surface of Mars. For example, CRISM data were recently used to observe an unexpected asymmetric springtime retreat of CO₂ ice observed in the north polar cap, potentially due to H₂O ice sourced from the north polar cap outliers (Brown et al., 2012). CRISM has also been used to examine Rayleigh scattering in the Martian atmosphere

(Brown, 2014) and to discriminate water and CO₂ ice deposited in halos around Swiss-cheese deposits (Becerra et al., 2014). Here we present CRISM observations of the south polar cap over four Martian years that show that surficial H₂O ice reappears each year on a repeatable and cyclic basis on the residual CO₂ ice cap throughout the austral summer. The increases in H₂O deposition occur across the entire SPRC but not in dusty or regolith-dominated regions beyond it.

Placing limits on the modern day deposition rate of water ice on the SPRC will allow us to better understand the modern-day stability of the southern polar cap (Byrne, 2009) and perhaps even shed light on the formation processes on the south polar cap (Montmessin et al., 2007). Many simulations of the Martian water cycle have investigated the question of cold-trapped water ice on the exposed CO₂ ice (Jakosky, 1983; Haberle and Jakosky, 1990; Houben et al., 1997; Richardson and Wilson, 2002; Montmessin et al., 2004; Montmessin et al., 2007) and we conclude the paper by comparing their predictions with our multiyear CRISM measurements.

2. Methods

Our primary means of monitoring the SPRC H₂O ice cycle comes from mosaics and spectra constructed of the CRISM global mapping data during Mars Year (MY) 28-31. The Compact Reconnaissance Imaging Spectrometer for Mars (CRISM) is a visible to near-infrared spectrometer on Mars Reconnaissance

Orbiter (MRO) spacecraft that is sensitive to near infrared (NIR) light from ~0.39 to ~3.9 μm and is operated by the Applied Physics Laboratory at Johns Hopkins University. We used the multispectral (MSP and HSP) TRR3 I/F data that are available from the Planetary Data System (PDS).

In CRISM mapping mode 10x on-instrument binning is employed in the cross-track direction. Consequently the mapping swathes we use are 60 pixels across, covering approximately 10.8 km on the surface (Murchie et al., 2007) with a down and cross track resolution of ~182 m. The length of each swathe is controlled by exposure time and is variable depending on commands sent to MRO.

We produced mosaics of all the CRISM mapping data available for each two-week period (equivalent to the time of an MRO planning cycle and also a useful cadence for investigating seasonal change in the Martian polar regions). Each mosaic is in polar-stereographic projection. Figure 1 shows the residual south polar ice cap region as a mosaic of CRISM images of the SPRC during the summer of MY28.

<insert Figure 1 here>

Water ice can be mapped on the surface using these near infrared mosaics by exploiting the 1.5 μm water ice absorption band. In Figure 2 we display a mosaic

map for early and late summer from MY 28, showing the presence of H₂O and CO₂ ice. We use a H₂O ice index first used by Langevin et al. (2007) and adjusted for use with CRISM by Brown et al. (2010a). The formula for this index is:

$$H_2O_{index} = 1 - \frac{R(1.500)}{R(1.394)^{0.7} R(1.750)^{0.3}} \quad (1)$$

Where $R(\lambda)$ indicates the reflectance at the wavelength λ in μm . The index is high when the 1.5 μm water ice band is present and low when it is not, and it increases as larger grain water ice is present (Warren, 1982).

<insert Figure 2 here>

3. Results

3.1 Residual ice cap mosaics

The first line of evidence for H₂O ice deposition is the residual cap ice identification maps in Figure 2. Following previous studies (Brown et al., 2010a; Brown et al., 2012) we use a H₂O index threshold of 0.125 to indicate that surficial H₂O is present. CO₂ ice is detected using a band analysis routine described (Brown, 2006) and successfully applied by Brown et al. (Brown et al., 2008b; Brown et al., 2010b). As in previous studies (Brown et al., 2010a; Brown et al., 2012), positive identification of CO₂ ice is indicated by a threshold 1.435 μm band depth of 0.16.

The ice identification maps show almost complete coverage of the residual cap in CO₂ ice (shown in red) and little to no H₂O ice in the early summer period (L_s=310). On the right of Figure 2, we have superposed the CRISM observations in the L_s=310-330 time period. These show strips of cyan where CRISM has detected small but significant increases in the 1.5 H₂O μm band. As can be seen from the CRISM mosaics in Figure 2, the effect is confined sharply to the south polar cap, and does not extend beyond the SPRC edge.

<insert Figure 3 here>

3.2 CRISM Reflectance Spectra

Our second line of evidence is taken from spectra extracted from a point within these maps. Figure 3 shows a set of individual CRISM MSP spectra (no averaging or binning has been done) prior to H₂O ice deposition (starting at L_s=261) and throughout summertime (finishing at L_s=337) from 265.5°E, 86.1°S (marked as Point A on Figure 1). The spectra show a marked decrease in the 1.5 μm band that causes a decrease in the shoulder of the CO₂ ice absorption band at 1.4 μm. As in previous studies (Brown et al., 2008a; Brown et al., 2010a; Brown et al., 2012) we attribute this change in band depth to the presence of increasing amounts of H₂O ice through the summer season.

<insert Figure 4 here>

3.3 Point observations at Point A and B

Our third line of evidence comes from mapping observations taken by the CRISM instrument for MY28-31. In order to establish that this process is cyclic, we have extracted individual spectra from regions close to Point A and have plotted the H₂O ice and CO₂ ice index and also to the 1.2 μm albedo for these spectra in Figure 4a-c. Coverage in MY 29-31 is not quite as comprehensive, however in Figure 4d-f we show the same data for Point B, which is on the other side of the SPRC from Point A. Being closer to the south pole, the composition of the Point B region is dominated by CO₂ ice for the duration of summer, and smaller amounts of H₂O ice signature appear at this location. However, as for Point A, a definite H₂O ice cycle can be observed throughout summertime, indicated by a H₂O ice index that starts relatively low and increases steadily throughout summertime. Thus, we were able to establish that the H₂O index behaves in a similar manner (i.e. it increases) throughout the summer across the entire SPRC and for all Martian years for which we have data.

<insert Figure 5 here>

3.4 Radiative Transfer Model and Quantification of Water Ice Deposited

In order to quantify the amount of H₂O ice deposited on the south polar cap, we developed a radiative transfer model to reproduce the broad characteristics of a number of CRISM MSP spectra taken at Point A (see Figure 1). The CRISM spectra taken at L_s=337 (in late summer, after H₂O ice deposition) in MY28 and radiative transfer model spectra are shown in Figure 5.

We carried out the radiative transfer modeling using the model proposed by Shkuratov et al.(1999) which is a simplified 1-dimensional model that allows us to interpret the effect of H₂O ice as a contaminant in a CO₂ ice snowpack. As in past research (Brown et al., 2010a), we used a three component model (optical constants of CO₂ ice (Hansen, 2005), H₂O ice (Warren, 1984) and palagonite (Roush et al., 1991) as a Martian dust simulant) and attempted to fit the overall albedo and key band strengths of CO₂ ice and H₂O ice in the spectrum.

We carried out two modeling approaches in order attempt to place physical bounds on the amount of water ice deposited on the south polar cap. The two models adopted are:

- 1.) 'minimum apparent' model, and
- 2.) 'extrapolated' model

The 'minimum apparent' model attempts to find the smallest amount of water ice that could explain the observed water ice band, and as discussed in previous work (Brown et al., 2010a; Brown et al., 2012) this is the most robust way to interpret the observed CRISM spectra. The 'extrapolated' model makes additional assumptions in an effort to provide a reasonable best approximation to the depth of the H₂O ice deposits.

'Minimum apparent' model. To carry out the 'minimum apparent' interpretation, we used a newly developed iterative band-fitting routine based on previous band fitting algorithms (Brown, 2006) to generate a three-component mixture of CO₂, H₂O ice and dust that matched three components:

- 1.) the NIR albedo,

- 2.) the CO₂ ice band depths at 1.435 μm, and
- 3.) the doublet near 2.2 μm and H₂O ice band at 1.5 μm.

For the late summer spectrum in Figure 5, we found that the best spectral match was obtained for CO₂ ice grain size of ~4.25mm, (C_{CO_2} =85.7% by volume) H₂O ice grain size of ~ 0.2mm (C_{H_2O} =5.1%) and palagonite of ~0.35 mm (C_{dust} =9.2% by volume). We used a porosity (q-factor) of $q=0.3$, corresponding to 70% pores and 30% ice/dust. These results are summarized in Table 1.

Component	Reference	Best fit grain size (microns)	Best fit concentration
CO ₂ ice	Hansen (2005)	4252.7	0.857
H ₂ O ice	Warren (1984)	200.1	0.051
Palagonite (soil)	Roush et al. (1991)	354.9	0.092

Table 1 – Details of the best fit parameters for the CRISM spectrum in Figure 5. The fit was applied over the spectral range from 1.02-2.5 microns. In this range, using wavelengths from the CRISM MSP range, there are 42 bands. Over this range, the average absolute fitting error per band is 0.01659 for this best fit. The porosity was constrained to be 0.3 (30% ice, 70% vacant).

In order to estimate the ‘minimum apparent’ amount of water ice deposited, we make the simplest assumption that the thickness of the water ice layer is a minimum of the derived grain size diameter ($D_{H_2O}=0.2\text{mm}$ or $2 \times 10^{-7}\text{km}$) from the radiative transfer calculation. The physical justification for this is that the water ice must be optically detectable, and therefore at least one optical pathlength should be available for the passage of vertically propagating photons. The true situation will be far more complex. We make the obviously simplified assumptions that:

Observations of the H₂O ice cycle on summertime Martian south polar cap

- 1.) the residual SPRC has an approximate area of $A_{cap}=2 \times 10^5$ sq. km (Brown et al., 2010a),
- 2.) the SPRC is uniformly covered in summertime by a water ice layer, and
- 3.) that the H₂O ice is distributed in a 'checkerboard' fashion and occupies $C_{H_2O} \cdot q = 0.05 \cdot 0.3 = 0.015$ or 1.5% of this area.

With these three assumptions, the minimal amount of water ice observed would be determined by the following linear relationship:

$$volume_{H_2O} = A_{cap} C_{H_2O} D_{H_2O} q \quad (2)$$

therefore $volume_{H_2O-minimal\ apparent} = 2 \times 10^5 \cdot 0.05 \cdot 2 \times 10^{-7} \cdot 0.3 = 6 \times 10^{-4} \text{ km}^3$.

We regard this as a 'minimum apparent' estimate because it is likely that the deposit could be as thick as 10 grain diameters ($10 \cdot D_{H_2O}$).

Extrapolated estimate. The 'extrapolated' approach assumes that the water ice observed by CRISM is the top layer of a deeper deposit that extends ten grain diameters, which is a reasonable situation for this type of deposit. In this case, using:

$$volume_{H_2O-extrapolated} = A_{cap} C_{H_2O} 10 D_{H_2O} q \quad (3)$$

we find $volume_{H_2O-extrapolated} = 2 \times 10^5 \cdot 0.15 \cdot 6 \times 10^{-8} \cdot 0.3 = 6 \times 10^{-3} \text{ km}^3$.

These rather firm sounding numbers must be balanced with the fact that we have assumed that the entire SPRC is covered by the same amount of water ice,

whereas we know from observations that the western part of the polar cap is covered in more ice than the eastern part of the cap (Figure 2).

Nevertheless, assuming a Martian atmospheric H₂O ice budget of ~0.1 km³ (Christensen, 2006), the amount of water ice participating in this process will make up as much as 0.6% (at minimum, for 0.2mm thick ice deposit) to 6% (at maximum, for 2mm thick ice deposit) of the atmospheric Martian water budget. Note that we are not stating that 0.6-6% of the atmospheric water ice is being deposited on the cap, because we cannot be sure of the immediate source of the process. However, if the water ice is to be completely sourced from the atmosphere, then it would make up 0.6-6% of the current Martian atmospheric water budget.

4. Discussion

4.1 Comparison with previous hydrological models

Reference	Annual Water loss rate to south polar cap in grams	Total Annual Water loss rate to south polar cap in microns	Transport flux to southern polar cap
Jakosky and Farmer (1982)	4x10 ¹⁴ g (maximum)		
Jakosky (1983) p.37	1.4-4.1x10 ¹⁴ g		20-40%
Haberle and Jakosky (1990) (their Table 2)		100-800 (lost by north cap)	12-25%
Houben (1997) p.9078	2.5x10 ¹⁴ g or 0.25GT	500	12-25%
Richardson and Wilson (2002) (their "VS Study")	1.4x10 ¹⁴ g		7-14%
Montmessin et al. (2007) p.8		400	9.6-20%
This study	0.6-6x10 ¹³ (min app)		0.6 (min app)

Observations of the H₂O ice cycle on summertime Martian south polar cap

	1.2-12x10 ¹³ _(extrap)		6 _(extrap) %
--	---	--	-------------------------

Table 2 – Comparison of GCM model water loss to south polar cap amounts with the results of this study. For the purposed of calculating the transport flux, the estimated total atmospheric water content is estimated at 1-2 x10¹⁵ g.

We compare this estimate with previous Martian hydrological cycle models in Table 2. Jakosky and Farmer (1982) made the first upper estimate of the water that might be transported to the south polar cap by measuring the water vapor above the north polar cap using the MAWD instrument on the Viking orbiters. Jakosky (1983) developed a simplified circulation model that reproduced observations of the MAWD instrument and included a loss of water ice to the south polar cap and a regolith sink. Haberle and Jakosky (1990) used a simulation of the Martian north pole in the light of MAWD measurements to suggest that regolith was necessary in keeping the north polar cap stable. They provided an estimate of 0.1-0.8 mm of loss of water ice from the north polar water ice cap, which they used to put upper bounds on the amount deposited on the south polar cap. Houben et al. (1997) developed a simplified 3D climate model of the Martian water cycle which included transport between atmosphere and regolith. Richardson and Wilson (2002) reported the first use of a Martian GCM with a water ice cycle, with water ice treated as a trace component, and Montmessin et al. (2004) carried out a similar study including water ice clouds (with varying size distributions) with the LMD GCM.

Our estimates are smaller than the estimates of all GCM models, which may be due to the conservative approach taken to interpretation of our spectra. We consider this a first order estimate that will be refined as future observations are made of the summer south polar cap.

Montmessin et al. (2007) carried out a similar GCM-based simulation of the amount of water ice deposited on the south polar cap on current-day Mars and compared this to a model of water ice deposition during reversed perihelion. They suggested the water ice at the base of the SPRC was emplaced during reversed perihelion conditions.

Montmessin et al. (2007) used a symmetric model of the south polar cap and predicted that water ice deposition would correlate with latitude – hence greatest deposition is at the pole and smaller amounts of H₂O ice would be deposited at the edge of the cap. This is contrary to the CRISM observations reported here of deposition favoring the warmer western part of the cap, a trend which is also apparent in the OMEGA H₂O ice maps presented by Langevin et al. (2007) (their Figure 18-19).

These observational versus simulation discrepancies indicate to us that future mesoscale modeling of this season is required. At the very least, higher resolution hydrological simulations with a realistic cap orientation should be used to help interpret the observed western depositional pattern on the south polar cap under modern Martian conditions.

4.2 Interannual differences

During MY28 there was a global dust storm (James et al., 2010) that induced a decrease in the albedo of the polar ice and subdued the H₂O and CO₂ ice signatures across the SPRC. This explains the relatively low MY28 index values seen in Figure 4. We have looked for evidence of larger amounts of H₂O ice being deposited each year but the evidence is inconclusive thus far.

4.3 Seasonal changes

The data presented in Figure 2 suggest that the depositional process is gradual and lasts all summer long, rather than being due to isolated or singular depositional events each summer. Close to Point A, H₂O index values start around 0.02 near L_s=275 and climb to greater than 0.275 at the end of summer for MY29-31. At Point B, which is nearer to the pole, the H₂O index values start around 0.02 near L_s=275 and climb to around 0.2 for MY29-31.

4.4 Deposition or Exposure of H₂O ice?

It should be noted that the spectra in Figure 3 show CO₂ ice and weak H₂O ice signatures mixed together in the same pixel. The mixing might be 'checkerboard' linear mixing or intimate mixing where CO₂ ice and H₂O ice grains are encountered by a single photon traversing the Martian snowpack. Therefore, it is not possible for us to tell definitively whether the observed H₂O ice cycle is a process of:

- 1.) **deposition** of H₂O ice on top of the SPRC (cold trapping)

2.) **sublimation** of CO₂ ice, revealing stratigraphically older H₂O ice mixed within the CO₂ snowpack.

3.) **atmospheric condensation** of H₂O ice particles within a sublimation flow above the CO₂ snowpack.

Option 1 (**deposition**) is our favored explanation for the observations reported here. Thermally thick (e.g. decimeter to meter thick) water ice units have been observed at the periphery and immediate vicinity of the SPRC during the summer following the sublimation of the last seasonal CO₂ ice (Titus et al., 2003; Piqueux et al., 2008) and the spectral signature of water ice was also observed by Bibring et al., (2004), on the SPRC mixed with CO₂ ice. Titus (2005) pointed out that it is also possible that H₂O ice might be deposited on top of the CO₂ ice cap during summertime, thus obscuring a large region of the CO₂ ice on the cap. Potential support for this interpretation is the observation that the water ice index is higher in the western regions of the cap, close to where H₂O ice is exposed in the sides of gullies (Titus, 2005).

Option 2 (**sublimation**) is considered less favorable since the weight of GCM modeling suggests that conditions are right for cold trapping of water vapor at this time. The truth may lie between these extremes – water ice may be exposed by CO₂ ice sublimation, and then transported to nearby cold trap locations (e.g. tops of ‘Swiss-cheese’ mesas) where it obscures the underlying CO₂ ice. This process may play a role in the burial of large amounts of CO₂ ice, which has been a key scientific question arising from the recent SHARAD radar sounder

findings of large amounts of CO₂ ice beneath the polar layered deposits (PLD) (Phillips et al., 2011).

Option 3 (**atmospheric condensation**) suggests that CRISM is collecting observations of a sublimation flow from the CO₂ polar cap during the height of summer, and that small H₂O crystals are forming within the sublimation flow as it evaporates off the ice pack. We consider this option less likely because of the increasing strength of the H₂O ice signature right through to fall – even as conditions begin to cool in late summer.

4.5 Atmospheric effects

For this study we have made no effort to remove atmospheric effects from the CRISM data. As mentioned above, a global dust storm was present in MY28 which affected the absorption band depths (Vincendon et al., 2008), however as can be seen in Figure 4, the H₂O cycle continued to operate in a similar manner to the following three Martian years. In addition, the water ice signatures appear only on the CO₂ ice cap (unlike the behavior of a cloud). We therefore infer that the H₂O ice cycle is present on the surface, and not due to an atmospheric event (Langevin et al., 2007). If the cycle is a depositional effect, (controlled by on-cap winds), stronger winds may play a role in the SPRC H₂O ice cycle, and this question invites future mesoscale climate modeling of the south polar region.

5. Conclusions

The source for the water ice reported here is unclear and we hope this study initiates new avenues of research for the Martian community. These findings impose an important constraint upon models of Martian water ice dynamics while opening a new front in the battle to understand the impoverished but vital Martian water ice cycle.

5.1. Stability of the SPRC

The operation of the H₂O ice cycle we have reported may have implications for the stability of the thin veneer of CO₂ ice that covers the residual south polar cap. Jakosky and Haberle (1990) suggested that the current CO₂ ice south polar residual cap is unstable and could 'flip' quickly to being covered by H₂O ice if water ice from the north polar cap makes its way to the southern cap, which acts as a cold trap in their model. As part of this cycle, and to explain observations of atmospheric H₂O observed above the south pole in 1969 (Barker et al., 1970), these authors suggested that the entire perennial CO₂ cap may have disappeared in the summer of 1969 (MY 8) and started to recondense shortly after. However, countering this suggestion, Thomas et al. (2005) used stratigraphic interpretations to date the oldest perennial cap unit as being ~100-150 MY old, excluding a complete removal of the cap in 1969.

Richardson and Wilson (2002) have also determined using GCM modeling that a H₂O ice south polar cap not covered by CO₂ ice is unstable under current Martian conditions and would disappear very quickly to the north polar cap.

The physics behind the energy balance of the polar ice cap is clear – in the near infrared (e.g. 1-4 μm) the presence of the H₂O ice layer we have reported here will lead to larger amounts of warming and degradation of the thin CO₂ ice veneer of the SPRC. A small amount of H₂O ice will absorb more sunlight in the 1-4 μm region (see Figure 3 showing decreasing near infrared albedo of the cap as H₂O index increases), causing more heating of the ice, and therefore more sublimation during the hottest part of the Martian orbital cycle.

5.2. CO₂-H₂O cycle is shown to be steady over 4 Mars years

It should be pointed out that as seen in Figure 4, for each Martian year observed, the CO₂ residual cap has been ‘re-coated’ during winter with CO₂ ice. This may have taken place by direct condensation or snowfall during the austral winter (Forget et al., 1998; Hayne et al., 2012; Hu et al., 2012; Hayne et al., 2013). We find ‘relatively pure’ CO₂ ice at the start of each austral summer in our CRISM mosaics (Figure 2). This shows that this ‘re-coating’ process is cyclic and at least stable on observable time scales (Haberle and Jakosky, 1990).

The fact that ‘relatively pure’ seasonal CO₂ ice is present all over the cap indicates that the H₂O ice we see deposited each summertime is entirely interned, and presumably becomes a permanent thin layer within the southern CO₂ ice cap. This process may have played a role in forming the south polar layered deposits (SPLD) if they formed at a time when the SPRC was larger.

5.3: Varying emissivity of the South Perennial Cap

The albedo and emissivity of the south cap are two critically important parameters determining its stability in the current climate (Wood and Paige, 1992; Blackburn et al., 2009; Guo et al., 2010). A stable cap (able to survive the short but relatively warm southern Martian summers) is difficult to model and previous studies have used various combinations of CO₂ ice/dust albedo and emissivities (James and North, 1982; Warren et al., 1990; Hansen, 1999; Doute et al., 2006; Bonev et al., 2008; Kahre and Haberle, 2010; Pilorget et al., 2011; Pommerol et al., 2011; Kieffer, 2013). However, we have shown that the optical properties of the cap transition from “covered by CO₂ ice” to “CO₂ and H₂O ice mixture” in the course of the Martian austral summer, and future models of the cap albedo and emissivity can now take this variability into account.

5.4. The southern cap as a sink for the Martian water cycle

The Martian water cycle is crucial to the understanding of geodynamics of the atmosphere, surface and sub-surface (Clifford, 1993) of the planet. The results of this study show there is an increase in the H₂O ice signature on the south polar residual cap throughout summer, and is distributed predominantly on the western side of the cap. This runs contrary to the results of Montmessin et al. (Montmessin et al., 2007) who modeled a pole-symmetric cap and found that more water ice deposited in the pole, and less deposited on the periphery.

The source of the H₂O ice is uncertain at this stage, but we have proposed three non-exclusive possibilities:

- 1.) Non-local origin (e.g. transport from the north polar cap)
- 2.) Local aeolian origin (e.g. exposed water ice around the edges of the cap being blown into the interior and exposed water ice in 'Swiss-cheese' moats (Titus, 2005)).
- 3.) Local solid-state origin (e.g. sublimation of H₂O ice around the cap periphery or regolith and recondensation over the cold cap (the so-called 'Houben process' in springtime in the north pole (Houben et al., 1997; Brown et al., 2012)).

These three possibilities may all be part of the eventual explanation for this intriguing, widespread and repeatable Martian polar phenomenon.

Acknowledgements

We would like to thank the entire CRISM Team, particularly the Science Operations team at JHU APL. We also thank Ted Roush for supplying the palagonite optical constants and Franck Marchis and Peter Jenniskens and referees Yves Langevin and Francois Forget for helpful comments on the

manuscript. This investigation was partially funded by NASA Mars Data Analysis Program Grants NNX11AN41G and NNX13AJ73G administered by Mitch Schulte. Piqueux' contribution was carried out at the Jet Propulsion Laboratory, under a contract with the National Aeronautics and Space Administration.

REFERENCES

- Barker, E. S., et al., 1970. Mars: Detection of Atmospheric Water Vapor during the Southern Hemisphere Spring and Summer Season. *Science*. 170, 1308-1310.
- Becerra, P., et al., 2014. Transient Bright “Halos” on the South Polar Residual Cap of Mars: Implications for Mass-Balance. *Icarus*.
<http://dx.doi.org/10.1016/j.icarus.2014.04.050>.
- Bibring, J.-P., et al., 2004. Perennial water ice identified in the south polar cap of Mars. *Nature*. 428, 627-630.
- Blackburn, D. G., et al., 2009. Sublimation kinetics of CO₂ ice on Mars. *Planetary and Space Science*. 58, 780-791.
- Bonev, B. P., et al., 2008. Albedo models for the residual south polar cap on Mars: Implications for the stability of the cap under near-perihelion global dust storm conditions. *Planetary and Space Science*. 56, 181-193.
- Brown, A. J., 2006. Spectral Curve Fitting for Automatic Hyperspectral Data Analysis. *IEEE Transactions on Geoscience and Remote Sensing*. 44, 1601-1608.
- Brown, A. J., et al., 2008a. Louth Crater: Evolution of a layered water ice mound. *Icarus*. 196, 433-445.
- Brown, A. J., et al., 2008b. The MARTE Imaging Spectrometer Experiment: Design and Analysis. *Astrobiology*. 8, 1001-1011.
- Brown, A. J., et al., 2010a. Compact Reconnaissance Imaging Spectrometer for Mars (CRISM) south polar mapping: First Mars year of observations. *Journal of Geophysical Research*. 115, doi:10.1029/2009JE003333.
- Brown, A. J., et al., 2010b. Hydrothermal formation of Clay-Carbonate alteration assemblages in the Nili Fossae region of Mars. *Earth and Planetary Science Letters*. 297, 174-182.
- Brown, A. J., et al., 2012. Compact Reconnaissance Imaging Spectrometer for Mars (CRISM) north polar springtime recession mapping: First 3 Mars years of observations. *Journal of Geophysical Research*. 117, E00J20.

- Brown, A. J., 2014. Spectral bluing induced by small particles under the Mie and Rayleigh regimes. *Icarus*. DOI: 10.1016/j.icarus.2014.05.042.
- Byrne, S., Ingersoll, A., 2003. A Sublimation Model for Martian South Polar Ice Features. *Science*. 299, 1051 - 1053.
- Byrne, S., 2009. The Polar Deposits of Mars. *Annual Review of Earth and Planetary Sciences*. 37, 535-560.
- Christensen, P. R., 2006. Water at the Poles and in Permafrost Regions of Mars. *Geoscience Elements*. 2, 151-155.
- Clifford, S. M., 1993. A Model for the Hydrologic and Climatic Behavior of Water on Mars. *Journal of Geophysical Research-Planets*. 98, 10973-11016.
- Doute, S., et al., 2006. South Pole of Mars: Nature and composition of the icy terrains from Mars Express OMEGA observations. *Planetary and Space Science*. 55, 113-133.
- Farmer, C. B., et al., 1976. Mars: Northern Summer Ice Cap—Water Vapor Observations from Viking 2. *Science*. 194, 1339-1341.
- Forget, F., et al., 1998. CO₂ Snowfall on Mars: Simulation with a General Circulation Model. *Icarus*. 131, 302-316.
- Guo, X., et al., 2010. On the mystery of the perennial carbon dioxide cap at the south pole of Mars. *Journal of Geophysical Research*. 115, E04005.
- Haberle, R. M., Jakosky, B. M., 1990. Sublimation and transport of water from the north residual polar cap on Mars. *Journal of Geophysical Research*. 95, 1423-1437.
- Hansen, G. B., 1999. Control of the radiative properties of the Martian polar caps by surface CO₂ ice: Evidence from Mars Global Surveyor measurements. *Journal of Geophysical Research*. 104, 16471-16486.
- Hansen, G. B., 2005. Ultraviolet to near-infrared absorption spectrum of carbon dioxide ice from 0.174 to 1.8 μm . *Journal of Geophysical Research*. 110, E11003.
- Hayne, P. O., et al., 2012. Carbon dioxide snow clouds on Mars: South polar winter observations by the Mars Climate Sounder. *Journal of Geophysical Research*. 117, E08014.
- Hayne, P. O., et al., 2013. The role of snowfall in forming the seasonal ice caps of Mars: Models and constraints from the Mars Climate Sounder. *Icarus*. 231, 122-130.
- Houben, H., et al., 1997. Modeling the Martian seasonal water cycle. *Journal of Geophysical Research-Planets*. 102, 9069-9083.
- Hu, R., et al., 2012. Mars atmospheric CO₂ condensation above the north and south poles as revealed by radio occultation, climate sounder, and laser ranging observations. *Journal of Geophysical Research*. 117, E07002.
- Jakosky, B., M., 1983. The role of seasonal reservoirs in the Mars water cycle: II. Coupled models of the regolith, the polar caps, and atmospheric transport. *Icarus*. 55, 19-39.
- Jakosky, B. M., Farmer, C. B., 1982. The Seasonal and Global Behavior of Water Vapor in the Mars Atmosphere: Complete Global Results of the Viking Atmospheric Water Detector Experiment. *Journal of Geophysical Research*. 87, 2999–3019.
- Jakosky, B. M., Haberle, R. M., 1990. Year-to-Year Instability of the Mars South Polar Cap. *Journal of Geophysical Research*. 95, 1359-1365.

- James, P. B., North, G. R., 1982. The seasonal CO₂ cycle on Mars - an application of an energy balance climate model. *Journal of Geophysical Research*. 87, 10271-10283.
- James, P. B., et al., 2010. Variability of the south polar cap of Mars in Mars years 28 and 29. *Icarus*. 208, 82-85.
- Kahre, M. A., Haberle, R. M., 2010. Mars CO₂ cycle: Effects of airborne dust and polar cap ice emissivity. *Icarus*. 207, 648-653.
- Kieffer, H. H., 1979. Mars South Polar Spring and Summer Temperatures: A Residual CO₂ Frost. *Journal of Geophysical Research*. 84, 8263-8288.
- Kieffer, H. H., et al., 2000. Mars south polar spring and summer behavior observed by TES: Seasonal cap evolution controlled by frost grain size. *Journal of Geophysical Research-Planets*. 105, 9653-9699.
- Kieffer, H. H., 2013. Thermal model for analysis of Mars infrared mapping. *Journal of Geophysical Research: Planets*. n/a-n/a.
- Langevin, Y., et al., 2007. Observations of the south seasonal cap of Mars during recession in 2004–2006 by the OMEGA visible/near-infrared imaging spectrometer on board Mars Express. *Journal of Geophysical Research*. 112, 10.1029/2006JE002841.
- Malin, M. C., et al., 2001. Observational evidence for an active surface reservoir of solid carbon dioxide on Mars. *Science*. 294, 2146-2148.
- Montmessin, F., et al., 2004. Origin and role of water ice clouds in the Martian water cycle as inferred from a general circulation model. *Journal of Geophysical Research*. 109, doi:10.1029/2004JE002284.
- Montmessin, F., et al., 2007. On the origin of perennial water ice at the south pole of Mars: A precession-controlled mechanism? *Journal of Geophysical Research*. 112, doi:10.1029/2007JE002902.
- Murchie, S., et al., 2007. Compact Reconnaissance Imaging Spectrometer for Mars (CRISM) on Mars Reconnaissance Orbiter (MRO). *Journal of Geophysical Research*. 112, E05S03, doi:10.1029/2006JE002682.
- Nye, J. F., et al., 2000. The Instability of a South Polar Cap on Mars Composed of Carbon Dioxide. *Icarus*. 144, 449-455.
- Phillips, R. J., et al., 2011. Massive CO₂ Ice Deposits Sequestered in the South Polar Layered Deposits of Mars. *Science*. 332, 838-841.
- Pilorget, C., et al., 2011. Dark spots and cold jets in the polar regions of Mars: new clues from a thermal model of surface CO₂ ice. *Icarus*. 213, 131-149.
- Piqueux, S., et al., 2008. Distribution of the ices exposed near the south pole of Mars using Thermal Emission Imaging System (THEMIS) temperature measurements. *Journal of Geophysical Research*. 113, doi:10.1029/2007JE003055.
- Pommerol, A., et al., 2011. Evolution of south seasonal cap during Martian spring: Insights from high-resolution observations by HiRISE and CRISM on Mars Reconnaissance Orbiter. *Journal of Geophysical Research: Planets*. 116, E08007.
- Richardson, M. I., Wilson, R. J., 2002. Investigation of the nature and stability of the Martian seasonal water cycle with a general circulation model. *Journal of Geophysical Research-Planets*. 107, art. no.-5031.
- Roush, T., et al., 1991. Derivation of Midinfrared (5–25 micrometer) Optical Constants of Some Silicates and Palagonite. *Icarus*. 94, 191-208.

- Shkuratov, Y., et al., 1999. A Model of Spectral Albedo of Particulate Surfaces: Implications for Optical Properties of the Moon. *Icarus*. 137, 235-246.
- Thomas, P. C., et al., 2005. South polar residual cap of Mars: Features, stratigraphy, and changes. *Icarus*. 174, 535-559.
- Titus, T. N., et al., 2003. Exposed water ice discovered near the south pole of Mars. *Science*. 299, 1048-1051.
- Titus, T. N., 2005. Thermal infrared and visual observations of a water ice lag in the Mars southern summer. *Geophysical Research Letters*. 32, doi:10.1029/2005GL024211.
- Titus, T. N., et al., 2008. Martian polar processes. In: J. F. Bell, (Ed.), *The Martian Surface: Composition, Mineralogy, and Physical Properties*. Cambridge University Press, pp. 578-598.
- Vincendon, M., et al., 2008. Dust aerosols above the south polar cap of Mars as seen by OMEGA. *Icarus*. 196, 488-505.
- Warren, S. G., 1982. Optical properties of snow. *Reviews of Geophysics*. 20, 67-89.
- Warren, S. G., 1984. Optical constants of ice from the ultraviolet to the microwave. *Applied Optics*. 23, 1206-1225.
- Warren, S. G., et al., 1990. Spectral albedo and emissivity of CO₂ in Martian polar caps: model results. *Journal of Geophysical Research*. 95, 14717-14741.
- Wood, S. E., Paige, D. A., 1992. Modeling the Martian seasonal CO₂ cycle 1. Fitting the Viking Lander pressure curves. *Icarus*. 99, 1-14.

FIGURES AND CAPTIONS

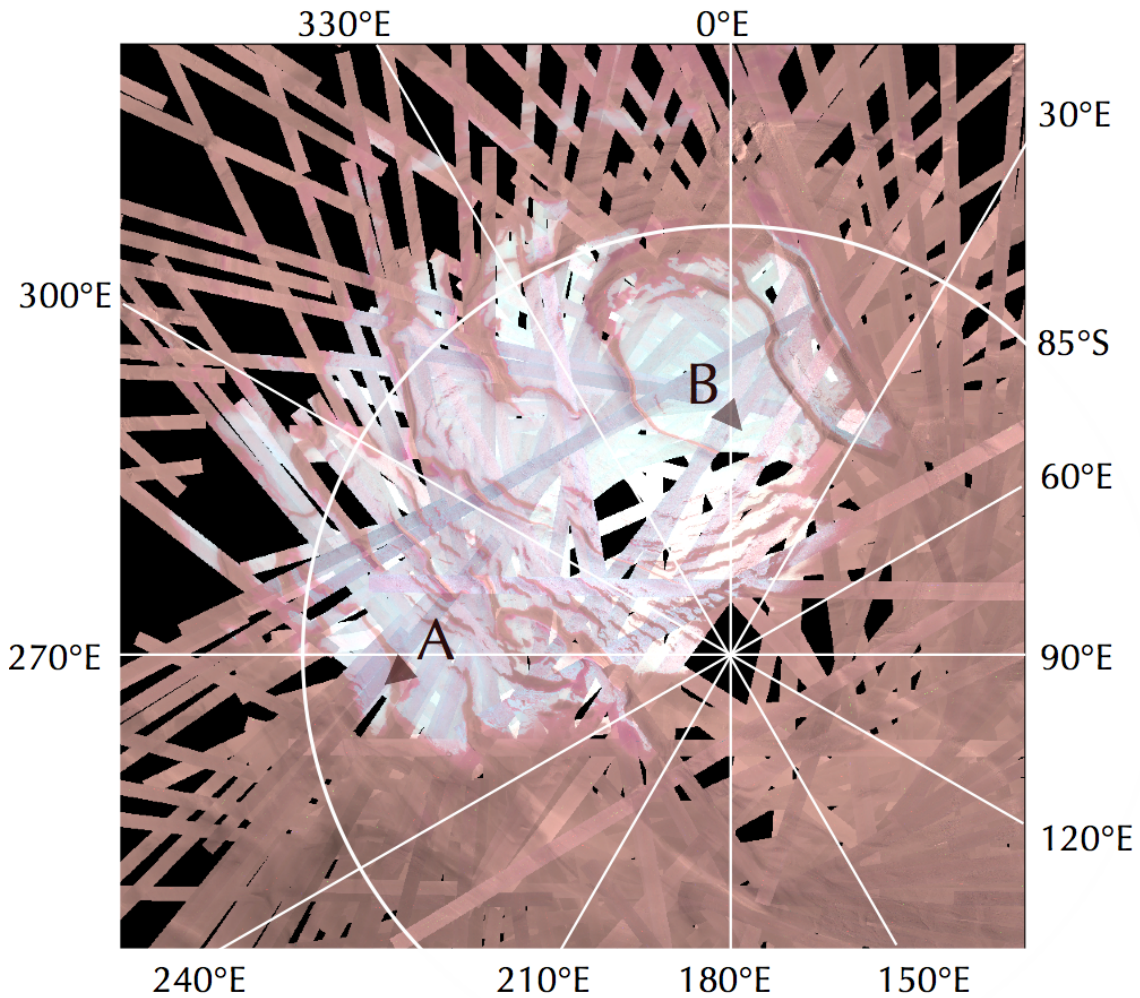


Figure 1 – CRISM mosaic of south polar residual cap (SPRC) in Mars Year 28, compiled during aerocentric longitude $L_s=304-319$ (mid summer) using three CRISM L channel bands (Red: 1.467, Green: 1.427 and Blue: 1.276 m). The locations of Point A (265.5°E, 86.1°S) and Point B (1.0°E, 87.0°S) are shown.

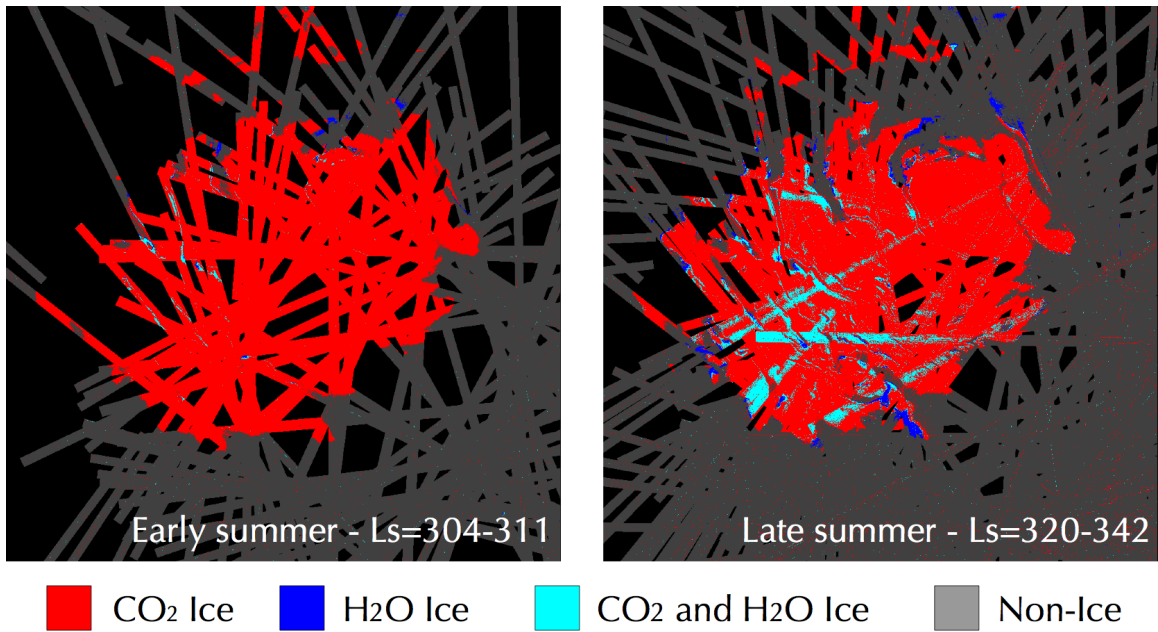


Figure 2 – Martian Year 28 southern summer ice identification mosaics. On left is the mosaic containing images from L_s=304-311. Note almost complete coverage by CO₂ ice (in red). On right is the mosaic constructed images spanning L_s=320-342. Note appearance of H₂O ice mixed with CO₂ ice in most recent images.

Summertime Evolution of CRISM Spectra at Point A

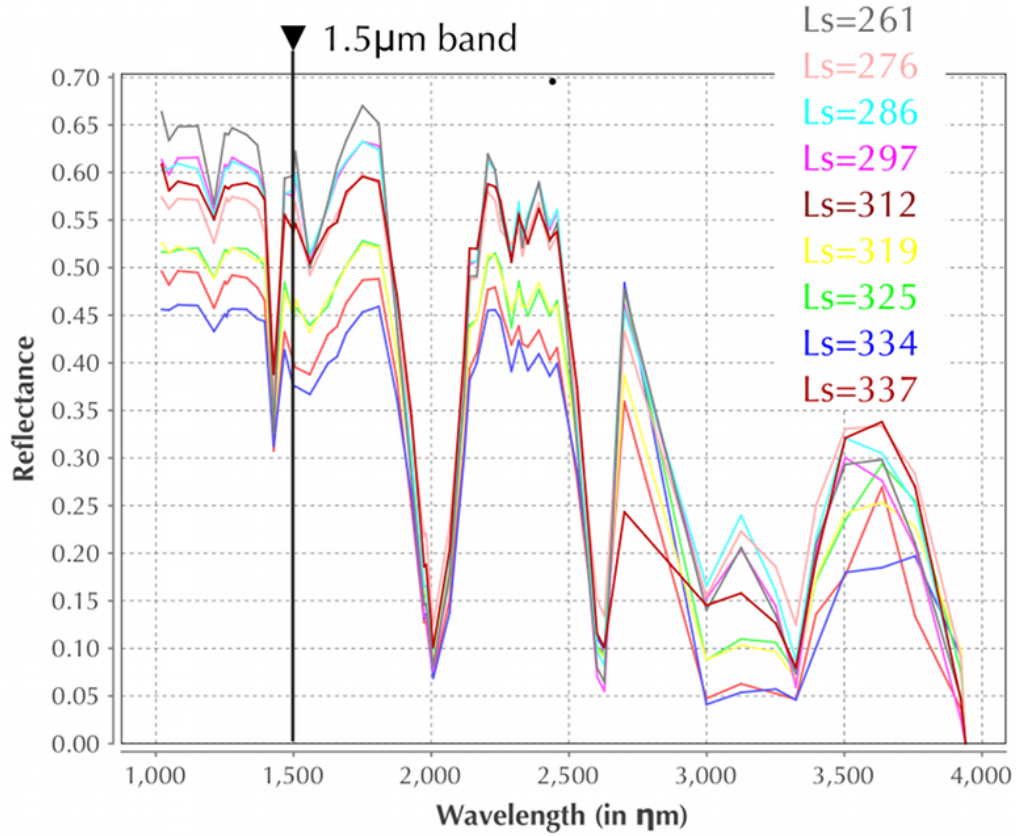


Figure 3 – CRISM summertime MSP spectra (from Point A in Figure 1) showing increase in H₂O ice absorption band for Mars Year 28 in late summer (pixels are ~180m across). The spectra were all taken close to Point A (265.5°E, 86.1°S; see Figure 1). Note overall decreasing albedo and increase in strength of H₂O absorption band at 1.5 μm throughout summertime.

Observations of the H₂O ice cycle on summertime Martian south polar cap

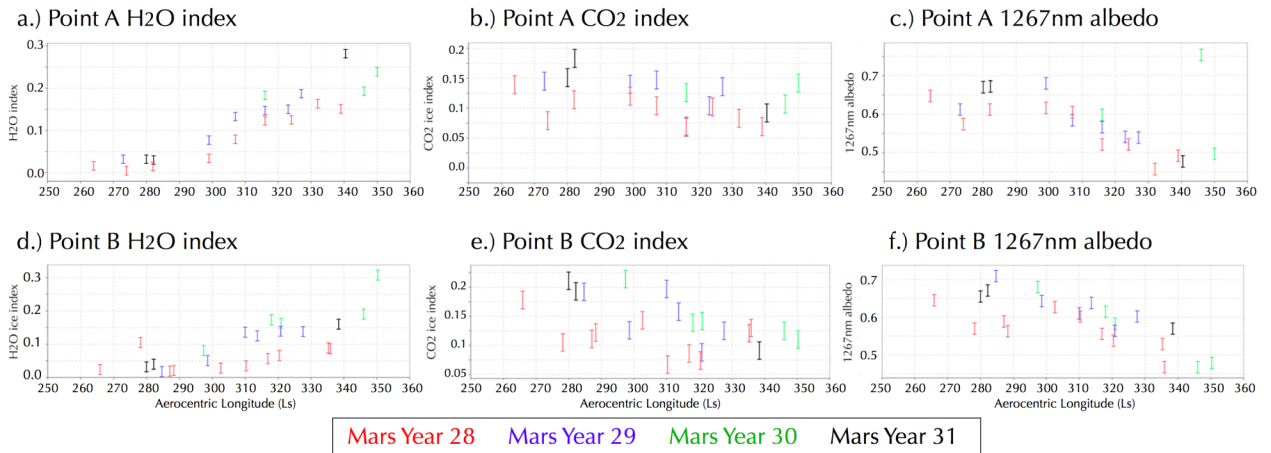


Figure 4a – CRISM H₂O ice index taken from points close to Point A from MY 28-31 during L_s=275-360 (austral summer). Note the increasing H₂O index during austral summer (from L_s=275-360) across all Mars years where data is available. Figure 4b-c – CRISM CO₂ ice index and CRISM 1.267 μm albedo at Point A during MY 28-31 during austral summer. Figure 4d-f – CRISM H₂O index, CO₂ index and 1.267 μm albedo for MY28-31 at Point B, located at (1°E, 87.0°S – see Figure 1).

Point A Late Summer spectrum vs. Model

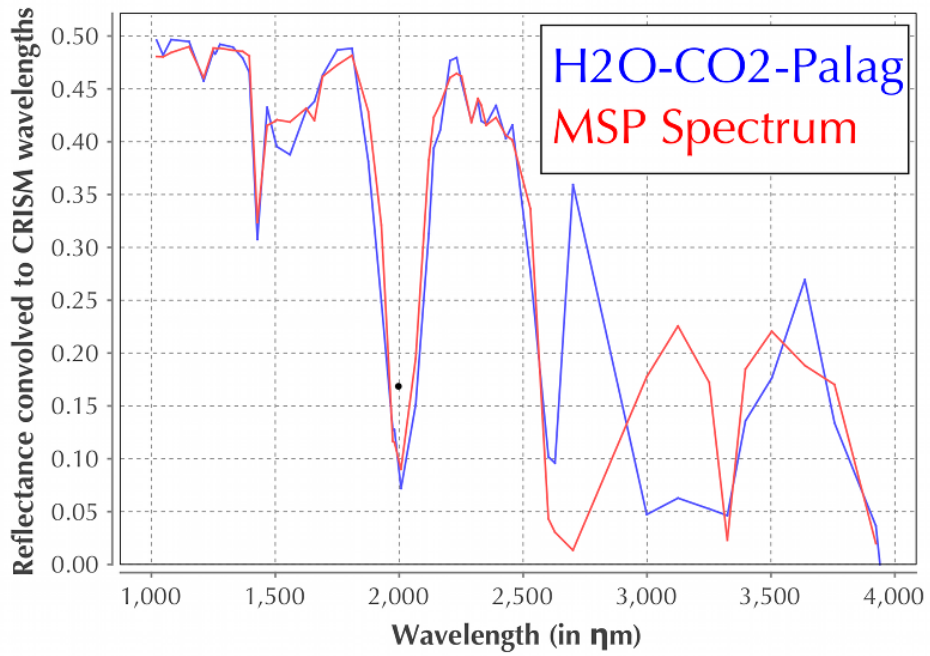


Figure 5 – Shkuratov reflectance models of CO₂, H₂O ice and palagonite mixture compared to CRISM L channel MSP spectra. See Table 1 for details of the fit. The CRISM spectra is sourced from Point A (see Figure 1) and was acquired in image MSP 86FC_01 on MY28 L_s=337.0 (26 Oct 2007).

SUPPLEMENTARY INFORMATION

In the course of this investigation, we used CRISM I/F data that had been processed by the CRISM team at JHU/APL to the TRR3 release level. Table A.1 shows the CRISM multispectral summer images that were taken of the Martian south pole from the start of the MRO mission to 27 June 2013.

	MRO Planning Cycle	DOY (2007-2013)	(MY) and L _s Range	S channel observations		L channel observations	
Mars Year 28	18	(07)172-181	261.5-267.1	234		232	
	19	188-198	271.5-277.8	346		346	
	20	199-212	278.4-286.5	199		200	
	21	213-219	287.1-290.8	123		125	
	22	227-240	295.6-303.4	119		118	
	23	241-254	304.0-311.6	146		146	
	24	255-268	312.2-319.7	210		210	
	25	269-282	320.2-327.5	180		180	
	26	283-296	328.1-335.2	172		173	
	27	297-309	335.7-342.1	152		150	
	Total			1881		1880	
Mars Year 29	28	350-352	(29) 3.1-4.1	26		26	
	29	353-001	4.6-10.9	183		183	
	30	(08)002-012	11.4-16.2	60		60	
	31	016-026	18.1-22.8	35		35	
	58	(09)113-125	252.4-260.0	43		43	
	59	127-138	260.9-268.4	42		42	
	60	140-153	269.3-277.5	59		59	
	61	154-167	277.9-286.3	27		26	
	62	168-179	286.7-293.5	28		28	
	63	184-192	296.4-301.6	65		66	
	64	196-209	303.7-311.6	117		116	
	65	210-223	312.0-319.7	39		39	
	66	224-237	319.8-327.6	174		174	
	67	238-238	327.6-327.7	7		7	
68	350-363	24.5-30.7	71		71		
69	364-(10)9	30.7-35.6	49		49		
70	013-013	37.2-37.3	3		3		
	Total			1028		1027	
Mars Year 30	91	(11)82-95	259.8-268.3	MSP	HSP	MSP	HSP
	92	99-100	270.8-271.2	32		31	
	93	114-116	279.8-281.6	2		2	
	94	128	288.7	12		12	
	95	142-145	297.0-298.8	1	8	1	8
	96	170-179	313.6-319.2	34	3	34	3
	97	180-183	319.5-321.3	16		16	
	98	226-235	344.4-349.4	1		1	
	99	236-239	349.7-351.5	81		81	
	101	282-290	(31)12.5-16.7	20		20	
	102	293	17.9	4		4	
		Total			203	11	202
Mars Year 31	123	(13)013-022	244.0-250.2	119		119	
	124	023-026	250.2-252.6	41		41	
	125	056	271.2	1		1	
	126	065-075	277.1-283.5	69	41	69	41
	127	167-176	336.4-341.6	32		32	
		Total			262	41	262

Table A.1 - CRISM observations of Mars south pole in the near-summertime from MY 28, L_s=260 to MY 31 L_s=342. L_s = Deg of solar longitude. Southern summer starts at L_s = 270 and ends at L_s = 360.

Locations and observation dates of the spectra shown in Figure 3:

Ls	MSP ID	MY	MRO Cycle	Earth Day
261.45	6508_01	28	18	2007_172 (21 Jun 07)
275.64	69F5_05	28	19	2007_194 (13 Jul 07)
285.85	6D6E_03	28	20	2007_210 (29 Jul 07)
296.49	7256_03	28	22	2007_228 (16 Aug 07)
311.67	79AA_01	28	23	2007_253 (10 Sep 07)
318.79	7D81_01	28	24	2007_266 (23 Sep 07)
324.60	8040_01	28	25	2007_276 (3 Oct 07)
333.67	850B_01	28	26	2007_293 (20 Oct 07)
337.0	86FC_01	28	27	2007_299 (26 Oct 07)

Table A.2 Locations and observation dates of the spectra shown in Figure 3.

Error bars on Figure 4a-f

Error bars are plotted as constant for the plots of 1267nm, CO₂ and H₂O ice index (Fig. 4a-f) as +/-0.015, based on the CRISM signal to noise (~100, based on data in Murchie et al. (Murchie et al., 2007)) for the 1.2-1.5 μm region.